

# Structural Approaches to Biomass Monitoring With Multibaseline, Multifrequency, Polarimetric Interferometry

*Robert N. Treuhaft\*, Beverly E. Law\*\*, and Gregory P. Asner\*\*\**

\*Jet Propulsion Laboratory, MS 138-212, California Institute of Technology  
4800 Oak Grove Drive, Pasadena, California 91109

Tel/Fax: 818-354-6216/818-393-5115 email: rnt@radar-email.jpl.nasa.gov

\*\*Department of Forest Science, Peavy Hall 154 Oregon State University, Corvallis, OR 97331

\*\*\*Department of Geological Sciences and Environmental Studies

Benson Earth Sciences Building, CB 399, University of Colorado, Boulder, CO 80309-0399

## 1. INTRODUCTION

One of the principal objectives of remote sensing is full carbon accounting in the world's forests via biomass monitoring. Determining carbon sequestration by forest ecosystems requires understanding the carbon budgets of these ecosystems, including carbon stored in plant mass above and below ground, and in soils. The net carbon uptake per year, which is related to the rate of change of biomass, is extremely important in long-term full carbon accounting. Foliage can account for up to 40% of the rate of change of biomass. The structure parameters estimated in this paper lead to two important components of biomass: 1) Wood biomass in the trunk and 2) upper-stem, branch, and foliage biomass. Wood biomass can be inferred from tree height, a parameter estimated in this paper [1], and diameter at breast height, which may be estimable from this work, but will probably require lower-frequency measurements, which may be more directly sensitive to trunk diameter [2]. The relative density profiles presented here, from which leaf area density can be calculated by additionally using hyperspectral data [3] will determine the foliage and branch biomass component, the monitoring of which is essential for measuring biomass rate of change.

Traditional, proposed approaches to microwave biomass measurement in forests rely on total power, at various polarizations, usually at frequencies of 400 MHz and lower [2]. Unlike the total-power data type, interferometric amplitudes and phases taken at sufficiently diverse baselines can uniquely estimate structural parameters such as forest height and scatterer-number-density profiles [4,5]; multifrequency and polarimetric interferometric observations further increase the accuracy and vertical spatial resolution of vegetation density profiles. In this paper, only single, vertical-polarization, multibaseline interferometry data were available at C- (5.6 cm) and L-band (24 cm),

along with full, noninterferometric polarimetry. The interferometric and polarimetric data at C-band yield Gaussian profile characteristics by using simple physical scattering models. The strategy for incorporating the acquired L-band data will also be discussed. The approach to modeling the fully polarimetric interferometric data, once they are acquired with AIRSAR or another airborne system, will also be discussed.

## 2. THE MULTIBASELINE, MULTIFREQUENCY INTERFEROMETRIC AND POLARIMETRIC DATA

The Jet Propulsion Laboratory's AIRSAR system acquired interferometric TOPSAR data [6] at three different altitudes, 8 km, 4 km, and 2 km over Central Oregon in the Metolius River Basin in April 1998. Because interferometric sensitivity is proportional to the baseline divided by the altitude [1], flying multiple altitudes is equivalent to acquiring multiple baselines. At each altitude, single-transmit and pingpong mode produced two baselines. The physical baseline is 2.45 m at C-band, and that is effectively doubled with pingpong mode. A redundancy was built into the acquisition strategy, because, for example 8 km pingpong interferometric data should be equivalent to 4 km single-transmit mode. Many systematic effects have been diagnosed using this redundancy. L-band interferometric were simultaneously acquired. Four race tracks were flown, three for interferometry, and one for C- and L-band zero-baseline polarimetry. The polarimetric interferometric data acquired in 1999 suffered from very poor signal-to-noise and must be reacquired in the future. Field measurements of tree height, height-to-base-of-crown, crown dimensions, and topography were made at each of 20 1-hectare stands. Profiling results will be compared to these field measurements.

### 3. MODELING VEGETATION PROFILE CHARACTERISTICS IN INTERFEROMETRY AND POLARIMETRY

The interferometric and polarimetric observations were related to vegetation parameters as indicated schematically below:

$$\begin{pmatrix} \text{Int Amp}_{8 \text{ km}} \\ \text{Int Phase}_{8 \text{ km}} \\ \text{Int Amp}_{8 \text{ km ping}} \\ \text{Int Phase}_{8 \text{ km ping}} \\ \text{Int Amp}_{4 \text{ km}} \\ \text{Int Amp}_{4 \text{ km ping}} \\ \text{Int Amp}_{2 \text{ km}} \\ \text{Int Amp}_{2 \text{ km ping}} \\ \text{Pol HHHH/VVVV} \end{pmatrix} = M \begin{pmatrix} \text{Veg Height} \\ \text{Peak Extinction} \\ \text{Density Center} \\ \text{Density std} \\ \text{Ground/vol} \\ \text{Gnd diel.} \\ \text{Topography} \end{pmatrix} \quad (1)$$

where "Int Amp" means interferometric amplitude, and the last entry in the observations on the left is the polarimetric horizontal to vertical power ratio. The reason for choosing this polarimetric quantity in the absence of polarimetric interferometry is detailed in [4]. A slightly-rough-surface approximation was necessary for this analysis, but could be generalized with polarimetric interferometry. The interferometric phases at the two lower altitudes were not used in this analysis because there is an indication of a bias introduced in processing, but this will be corrected shortly, and they will be used in future analyses. The physical model  $M$  relating the observations on the left of (1) to the parameters on the right relies on randomly oriented volumes over slightly-rough ground surfaces, and is also described in [4]. The extinction coefficient  $\sigma_x(z)$  is modeled with the parameters above as a Gaussian as a function of altitude  $z$ :

$$\sigma_x(z) = \text{Peak Extinction} \times \exp \left[ -\frac{(z - \text{Density Center})^2}{2(\text{Density std})^2} \right] \quad (2)$$

Because the extinction coefficient depends on the scatterer density, the density center and std (standard deviation) are assumed to describe a Gaussian density profile. This profile is also used to evaluate backscattering contributions to the interferometric and polarimetric data. The "ground/vol" parameter reflects the relative strength of the ground and volume scattering and depends on ground roughness backscattering strength. "Gnd diel." is the dielectric constant of the ground.

The L-band interferometric amplitudes and at 4- and 2-km altitudes and the polarimetry will be added to the parameter estimation scenario in (2). With nine additional L-band observations, two new parameters will have to be added, "Peak Extinction" and "Ground/vol" parameters for L-band. Assuming that all C-band phases will also

be used, the following parameter estimation scenario will then be tried, with subscripts denoting the band:

$$\begin{pmatrix} \text{Int Amp}_{8 \text{ km}_C} \\ \text{Int Phase}_{8 \text{ km}_C} \\ \text{Int Amp}_{8 \text{ km ping}_C} \\ \text{Int Phase}_{8 \text{ km ping}_C} \\ \text{Int Amp}_{4 \text{ km}_C} \\ \text{Int Phase}_{4 \text{ km}_C} \\ \text{Int Amp}_{4 \text{ km ping}_C} \\ \text{Int Phase}_{4 \text{ km ping}_C} \\ \text{Int Amp}_{2 \text{ km}_C} \\ \text{Int Phase}_{2 \text{ km}_C} \\ \text{Int Amp}_{2 \text{ km ping}_C} \\ \text{Int Phase}_{2 \text{ km ping}_C} \\ \text{Pol HHHH/VVVV}_C \\ \text{Int Amp}_{4 \text{ km}_L} \\ \text{Int Phase}_{4 \text{ km}_L} \\ \text{Int Amp}_{4 \text{ km ping}_L} \\ \text{Int Phase}_{4 \text{ km ping}_L} \\ \text{Int Amp}_{2 \text{ km}_L} \\ \text{Int Phase}_{2 \text{ km}_L} \\ \text{Int Amp}_{2 \text{ km ping}_L} \\ \text{Int Phase}_{2 \text{ km ping}_L} \\ \text{Pol HHHH/VVVV}_L \end{pmatrix} = M \begin{pmatrix} \text{Veg Height} \\ \text{Peak Extinction}_C \\ \text{Density Center} \\ \text{Density std} \\ \text{Ground/vol}_C \\ \text{Gnd diel.} \\ \text{Topography} \\ \text{Peak Extinction}_L \\ \text{Ground/vol}_L \end{pmatrix} \quad (3)$$

### 4. ESTIMATING VEGETATION PROFILE CHARACTERISTICS FROM THE DATA

Figure 1 shows three Gaussian profiles of scatterer number density for three forest stands, calculated from the first, third, and fourth parameters above. The profiles are relative in that the peak density for each stand is set to 1.0. Stand 1 is a mixed-height stand of Ponderosa Pine, with most trees about 12 m and a smaller number about 40 m. Stand 2 is old growth, of fairly uniform height of 40 m. Stand 3 is a young, dense stand about 15 m tall.

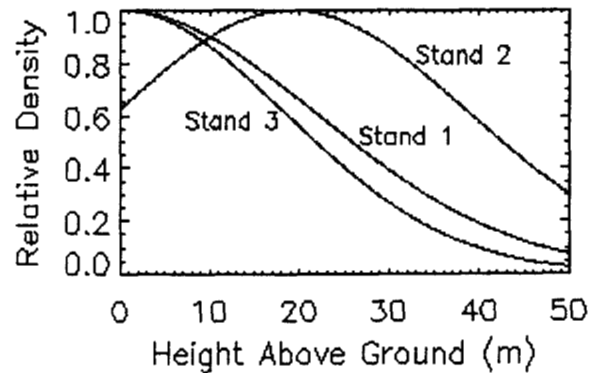


Figure 1: Relative Gaussian density profiles of three forest stands in Central Oregon from multi-altitude AIRSAR interferometry + polarimetry.

The profiles of Figure 1 exhibit qualitative agreement with field measurements, but show errors as well. For example, the estimated profile for stand 2 is broader than that for either stand 1 or stand 3, which is correct, but the estimated stand 3 profile, which has no tall component, should be substantially narrower than stand 1, which does. All three stands' densities extend beyond the actual maximum tree height. These errors could be indications of instrumental calibration errors and/or modeling errors. For example, if the actual profiles behaved more like two Gaussians than one, an artificially long tail might result from forcing the data to be fit by only one. Also, the slightly-rough-surface approximation, that surface roughness is less than a C-band 5.6-cm wavelength, may not be appropriate for this terrain. Fully polarimetric interferometry would obviate the need for this assumption [4].

Figure 2 shows the field-measured leaf-area-density along with the profile of stand 1, both arbitrarily normalized. In future analyses, AVIRIS-determined leaf-area-indices will normalize the profiles. Again, the agreement is reasonable, given that this is the first attempt to recover vegetation profiles from this type of data. The shape of

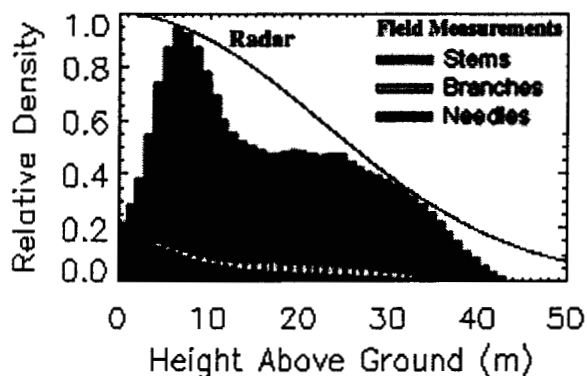


Figure 2: Relative Gaussian density profiles of Stand 1 from radar and leaf area densities from field measurements..

the radar-estimated profile is reasonably close to the field measurements. However, the parameter determining the radar cutoff vegetation height should have been closer to 40 m, and a shifted and narrower Gaussian would be a better fit to the field data. Some of the discrepancy is due to parameter estimate error, and some is due to systematic instrumental and modeling error. A full accounting of parameter estimate errors and the covariance between parameters will clarify how to improve Figure 2 with these and future data.

## 5. SUMMARY

Remote sensing of vegetation structure is an important component of biomass measurement and biomass rate-of-

change monitoring for full carbon accounting. A set of parameters describing Gaussian vegetation profiles were estimated from multialtitude AIRSAR interferometry, which is equivalent to multibaseline interferometry, plus zero-baseline polarimetry. The estimation involved a physical model of randomly oriented volumes and slightly-rough surfaces. While there is reasonable agreement between profiles estimated from radar and those measured in the field, both instrumental and modeling enhancements should improve this first attempt at estimating profiling parameters from interferometry and polarimetry.

## 6. ACKNOWLEDGMENT

We thank Ellen O'Leary, Anhua Chu, and the AIRSAR team for acquiring and special processing of the AIRSAR data. We also thank Scott Hensley for discussions on important systematic effects in the data. The research described in this paper was carried out in part by the Jet Propulsion Laboratory, California Institute of Technology, under contract with the National Aeronautics and Space Administration, NASA OES RTOP 622-93-63-40.

## 7. REFERENCES

- [1] R. N. Treuhaft, S. N. Madsen, M. Moghaddam, and J. J. van Zyl, "Vegetation Characteristics and Surface Topography from INSAR," *Rad. Sci.*, Vol. 31, 1996, pp. 1449-1485.
- [2] M. L. Imhoff, "Radar Backscatter and Biomass Saturation: Ramifications for Global Biomass Inventory," *IEEE Trans. Geosci. and Rem. Sens.*, Vol. 33, 1995, pp. 511-518.
- [3] G. P. Asner, C. A. Wessman, and D. S. Schimel, "Heterogeneity of savanna canopy structure and function from imaging spectrometry and inverse modeling," *Ecological Applications*, Vol. 8, 1998, pp. 926-941.
- [4] R. N. Treuhaft and P. R. Siqueira, "Vertical Structure of Vegetated Land Surfaces from Interferometric and Polarimetric Radar," *Radio Science*, vol. 35, 2000, pp. 141-177.
- [5] R. N. Treuhaft, M. Moghaddam, and B. Yoder, "Forest Vertical Structure from Multibaseline Interferometric Radar for Studying Growth and Productivity," *IGARSS97*, Singapore, 1997.
- [6] H. A. Zebker, S. N. Madsen, J. Martin, K. B. Wheeler, T. Miller, Y. Lou, G. Alberti, S. Vettorella, and A. Cucci, "The TOPSAR Interferometric Radar Topographic Mapping Instrument," *IEEE Transactions on Geoscience and Remote Sensing*, Vol. 30, 1992, pp. 933-940.